SUPPORTING INFORMATION for

Targeting RNA-Protein interactions within the HIV-1 lifecycle.

*Neil M. Bell,[1,2] Anne L'Hernault,[2] Pierre Murat,[1] James E. Richards,[2] Andrew M.L. Lever[2] & Shankar Balasubramanian[1,3]**

1) Department of Chemistry, University of Cambridge, Lensfield Rd, Cambridge, CB2 1EW, UK.
2) Department of Medicine, Addenbrooke's Hospital, University of Cambridge, Cambridge, CB2 0QQ, UK.
3) Cancer Research UK Cambridge Research Institute, Li Ka Shing Centre, Robinson Way, Cambridge, CB2 0RE, UK.

SUPPORTING RESULTS AND DISSCUSION

SUPPORTING FIGURES

SUPPORTING TABLES

SUPPORTING REFERENCES

SUPPORTING RESULTS AND DISSCUSION

The small molecule screen uses the increase in fluorescence intensity to monitor the rearrangement of an RNA molecular beacon substrate **FQ WT** (based on SL3 within the Ψ-packaging domain), upon binding of the Gag protein[1]. Small molecules that can prevent the unwinding of **FQ WT** either through the inhibition of Gag binding to or unwinding of the **FQ WT** will be detected by the low fluorescence intensity when compared to the negative control. Addition of unlabeled SL3 RNA to **FQ WT** prior to the addition of the gag polypeptide showed the **FQ WT**-Gag interaction could be inhibited and fluorescence intensity comparable to that of the **FQ WT** molecular beacon alone was achieved. For these reasons the **FQ WT** alone as well as SL3 were used as positive controls, (with SL3 being a “small molecule like” positive control set at 100% inhibition), DMSO alone was used as the negative control for the SM screen set at 0% inhibition.

The SM screening data was normalized as percentage inhibition of **FQ WT** relative to the positive and negative controls (Supp. Fig. 1); positive hits were defined as small molecules showing inhibition greater than three standard deviations (21%) from the mean negative control. On each plate, the controls were used to calculate the Z’ score and any plate which failed to gain a Z’ greater than 0.5 was rejected and the plate was rescreened. Confirmation of the primary hits was performed in triplicate under the original screening conditions.

SUPPORTING FIGURES

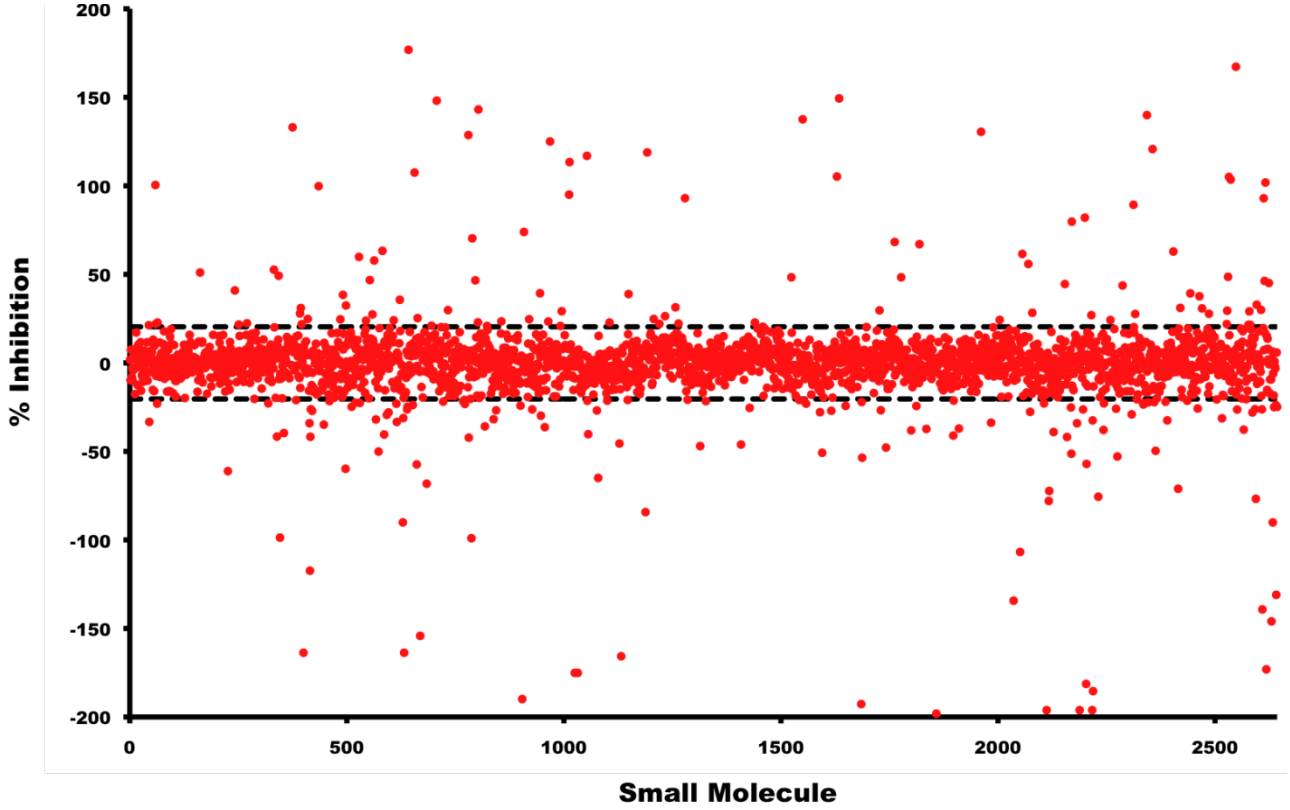

Figure S1: Results from the initial small molecule screen. Hits showing a positive inhibition of three standard deviations or more, from the negative control (dotted line), were validated by rescreening under the original conditions in triplicate.

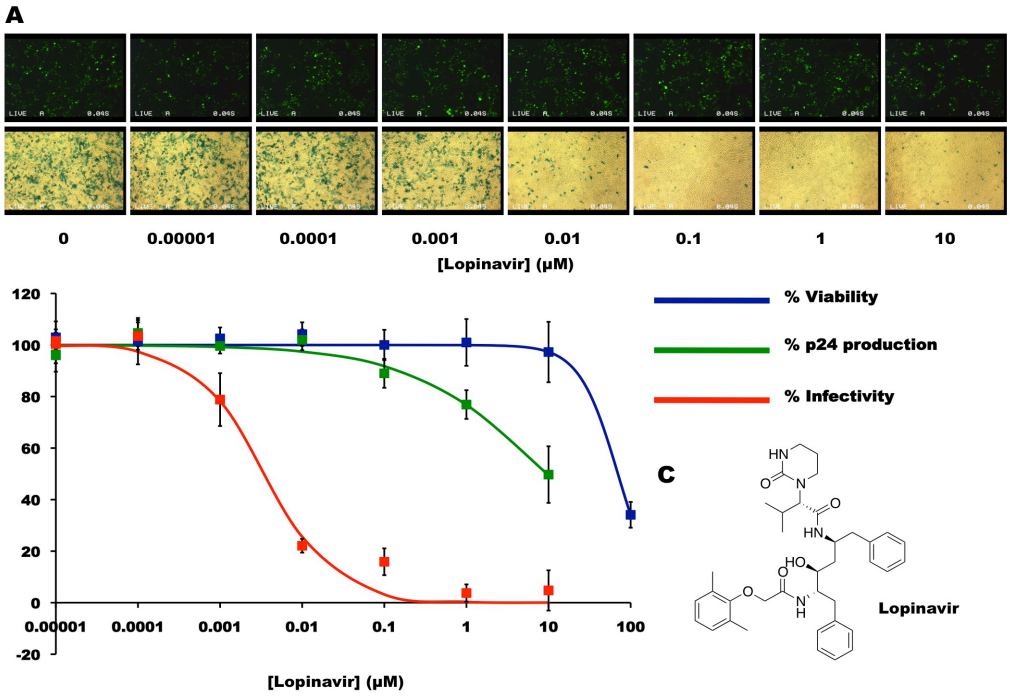

Figure S2 Biological activity of Lopinavir. **A**) 24 h post-infection the expression of β-galactosidase within the TZM-bl cell was imaged using X-Gal (bottom row). **B**) Viability of the 293T cells (blue line, 50% inhibition ($CC_{(50)}$ = 69.1 ± 15.3 µM)), viral production from transfected 293T (green line, 50% inhibition ($p24_{(50)}$ = 9.6 ± 3.2 µM)) and infectivity of harvested viral particles (red line 50% inhibition ($IC_{(50)}$ = 0.035 ± 0.008 µM)) in the presence of different concentrations of Lopinavir. **C**) Structure of Lopinavir

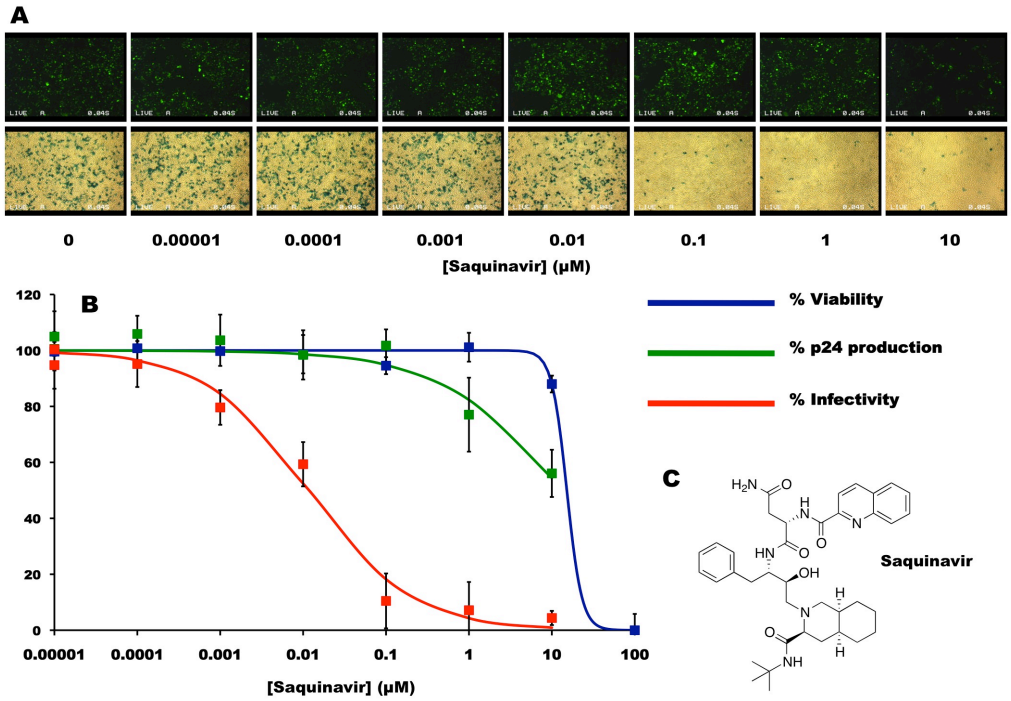

Figure S3: Biological activity of Saquinavir. **A**) 24 h post-infection, the expression of β-galactosidase within the TZM-bl cell was imaged using X-Gal (bottom row). **B**) Viability of the 293T cells (blue line, 50% inhibition ($CC_{(50)}$ = 15.1 ± 4.5 μM)), viral production from transfected 293T (green line, 50% inhibition ($p24_{(50)}$ = 13.5 ± 4.2 μM)) and infectivity of harvested viral particles (red line 50% inhibition ($IC_{(50)}$ = 0.011 ± 0.005 μM)) in the presence of different concentrations of Saquinavir. **C**) Structure of Saquinavir

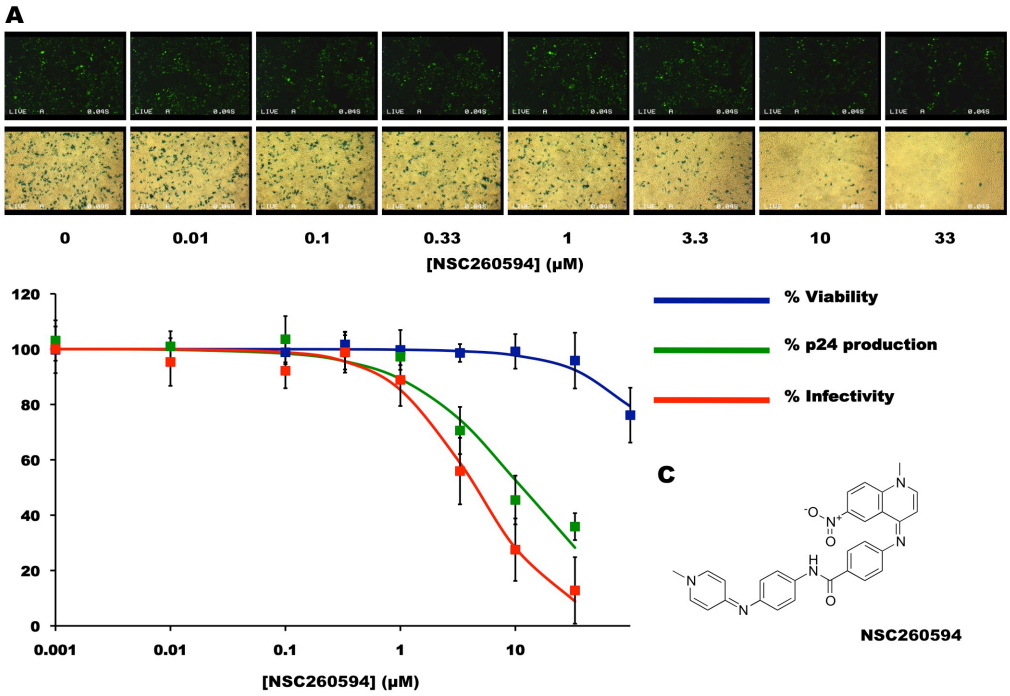

Figure S4: Biological activity of NSC260594. **A**) 24 h post-infection, the expression of β-galactosidase within the TZM-bl cell was imaged using X-Gal (bottom row). **B**) Viability of the 293T cells (blue line, 50% inhibition ($CC_{(50)}$ = N/A)), viral production from transfected 293T (green line, 50% inhibition ($p24_{(50)}$ = 11.3 ± 3.4 μM)) and infectivity of harvested viral particles (red line 50% inhibition ($IC_{(50)}$ = 4.5 ± 1.8 μM)) in the presence of different concentrations of NSC260594. **C**) Structure of NSC260594

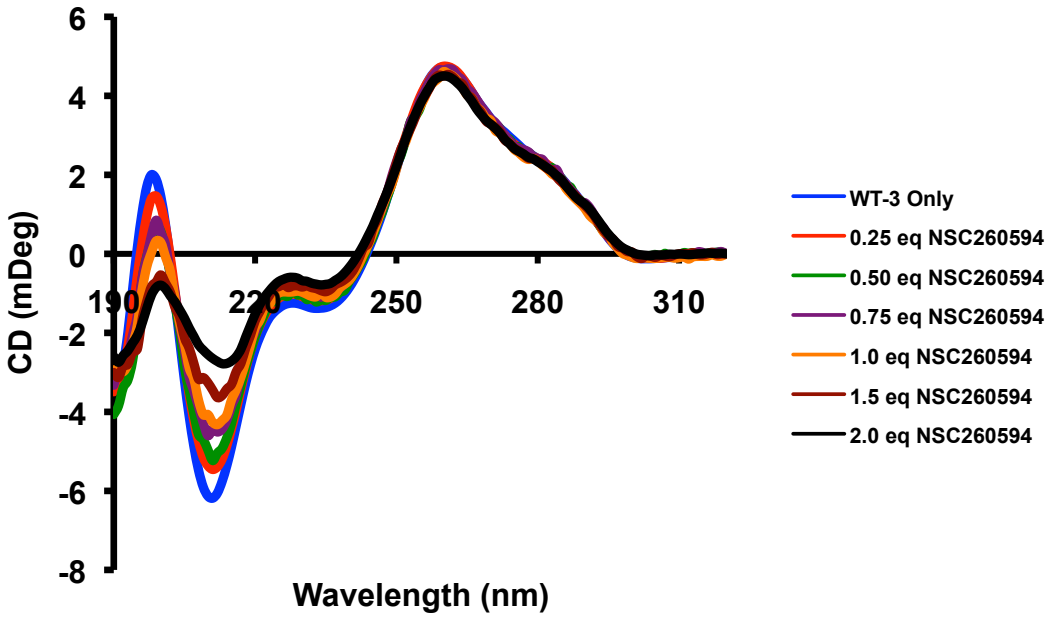

Figure S5: CD spectra of **WT-3** titrated against increasing amount of NSC260594. The decrease in CD signal at 210 nm and 195 nm with increasing concentrations of NSC260594 indicates a direct interaction between the molecule and the SL3 RNA.

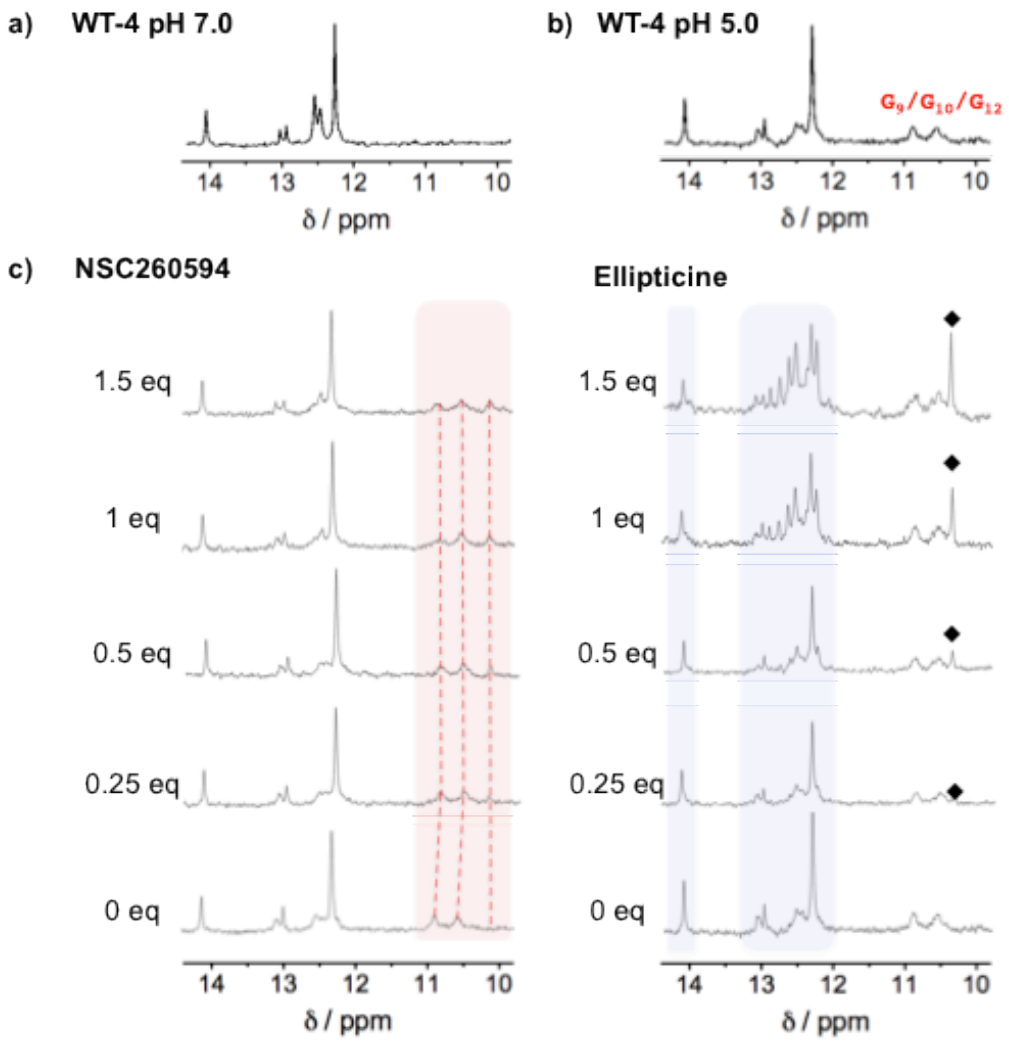

Figure S6: Imino proton NMR spectra of the titrations of a) NSC260594 and b) ellipticine against **WT-3** done at pH 5.0. The imino protons between 12 and 14.5 p.p.m (blue region) are attributed to the Watson-Crick H-bonded base pairs of the stem of the hairpin structure and imino protons between 10 - 11 p.p.m (red region) are attributed to the **WT-3** loop G bases. The black diamond (◆) highlights a peak attributed to ellipticine.

SUPPORTING TABLES

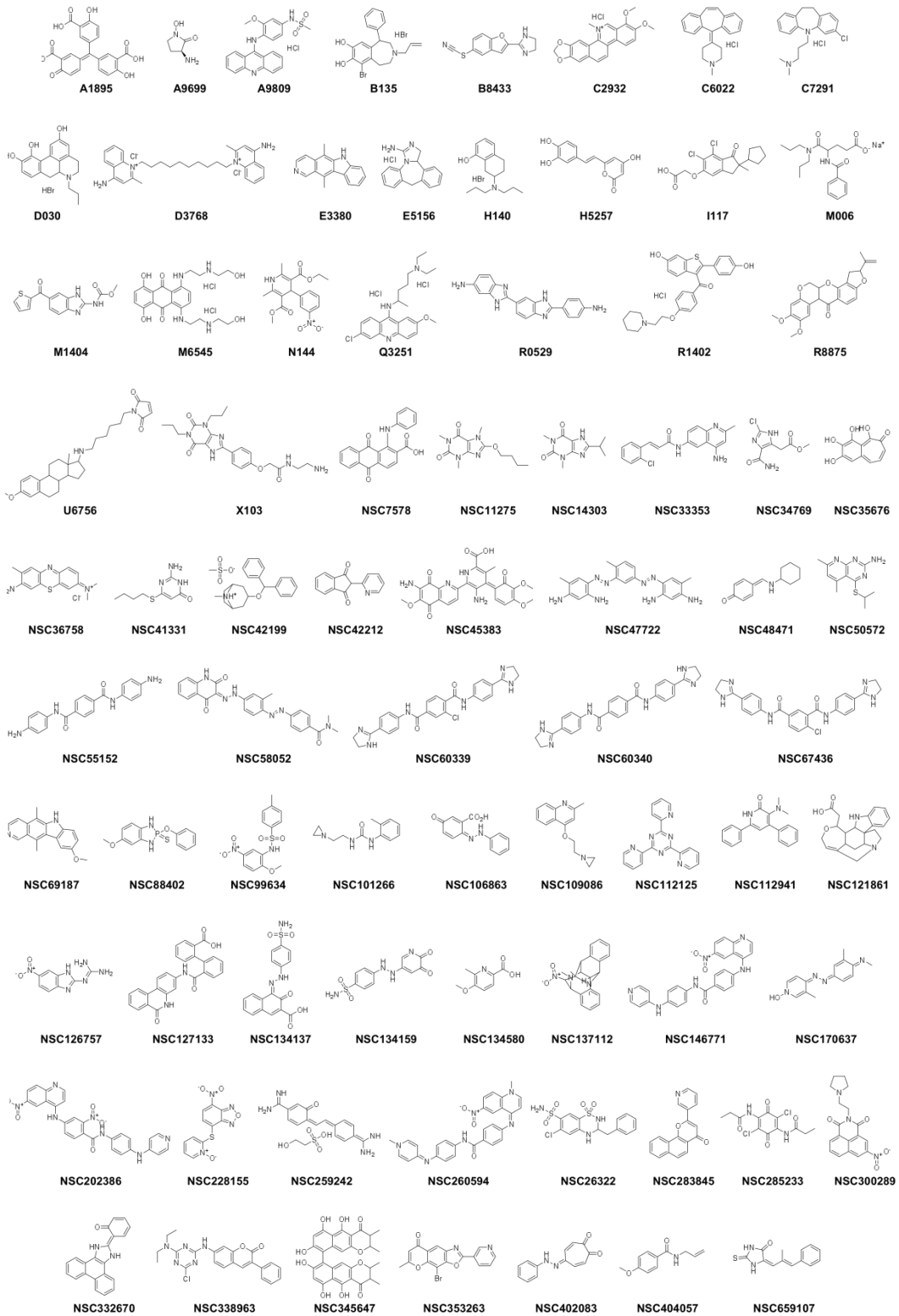

Table S1: Small molecules taken forward from the *in vitro* destablisation assay to the viral replications assays.

Compound	$CC_{(50)}$	SD	$IC_{(50)}$	SD
A1895	-	-	0.2	0.1
A9699	-	-	-	-
A9809	3.9	3.3	-	-
B135	24.2	3.4	-	-
B8433	37.9	4.9	6.7	3.5
C2932	2.7	0.5	-	-
C6022	16.6	2.2	-	-
C7291	20.7	11.3	8.4	5.2
D030	19.4	12.9	3.8	2.2
D3768	26.7	15.8	-	-
E3380	27.0	12.9	22.7	12.2
E5156	77.9	9.4	-	-
H140	0.6	0.4	-	-
H5257	27.9	3.2	7.4	2.8
I117	58.9	7.5	-	-
M006	-	-	-	-
M1404	-	-	-	-
M6545	0.9	0.4	-	-
N144	32.4	10.6	-	-
Q3251	3.0	1.6	-	-
R0529	-	-	13.9	8.0
R1402	17.1	2.3	-	-
R8875	3.0	0.9	-	-
U6756	29.2	14.5	-	-
X103	-	-	-	-
NSC7578	55.0	8.0	24.2	7.2
NSC11275	-	-	-	-
NSC14303	-	-	-	-
NSC33353	3.1	1.6	-	-
NSC34769	-	-	-	-
NSC35676	63.7	7.7	-	-
NSC36758	4.6	2.7	-	-
NSC41331	-	-	72.8	21.0
NSC42199	36.8	5.8	-	-
NSC42212	-	-	21.6	12.3
NSC45383	0.4	0.2	-	-
NSC47722	20.5	5.2	-	-
NSC48471	-	-	-	-

Compound	$CC_{(50)}$	SD	$IC_{(50)}$	SD
NSC50572	-	-	-	-
NSC55152	-	-	-	-
NSC58052	48.5	12.0	-	-
NSC60339	-	-	68.6	21.2
NSC60340	-	-	56.1	25.1
NSC67436	-	-	92.0	14.3
NSC69187	11.2	2.2	3.3	1.5
NSC88402	-	-	-	-
NSC99634	-	-	-	-
NSC101266	-	-	56.1	9.8
NSC106863	-	-	-	-
NSC109086	42.2	5.5	-	-
NSC112125	-	-	47.7	17.9
NSC112941	-	-	-	-
NSC121861	-	-	-	-
NSC126757	-	-	57.0	23.4
NSC127133	-	-	-	-
NSC134137	-	-	-	-
NSC134159	10.3	2.9	-	-
NSC134580	-	-	-	-
NSC137112	-	-	-	-
NSC146771	-	-	46.2	19.3
NSC170637	11.9	3.8	-	-
NSC202386	-	-	20.5	2.4
NSC228155	13.8	1.2	-	-
NSC259242	-	-	41.5	20.9
NSC260594	-	-	4.5	1.8
NSC263220	-	-	-	-
NSC283845	44.2	4.6	-	-
NSC285233	1.4	0.6	-	-
NSC300289	-	-	-	-
NSC317605	5.0	2.9	-	-
NSC332670	17.0	2.5	4.7	2.0
NSC338963	-	-	83.6	1.1
NSC345647	11.2	2.7	-	-
NSC353263	-	-	-	-
NSC402083	32.0	6.9	-	-
NSC404057	-	-	-	-
NSC659107	-	-	73.4	52.3

Table S2: Results from the viral replication assays to determine initial cytotoxicity and efficacy of potential hits from the initial small molecule screen.

[NSC260594] µM	0	0.5	1	5	10	20	30	40	50	100
T_m (°C)	85.7	85.8	85.5	86.1	86.7	88.4	<95	<95	<95	<95
SD	1.0	0.9	1.2	0.5	0.2	1.0	-	-	-	-
ΔT_m (°C)	-	0.11	-0.23	0.57	0.57	1.71	-	-	-	-

Table S3: Fluorescence melting titration of compound NSC260594 (0-100 µM) against the oligo **FQ WT** that was used in the initial *in vitro* screen. Above 20 µM of NSC260594 **FQ WT** becomes stablised and FQ WT can not be melted even at 95 °C.

SUPPORTING REFERENCES

(1) Bell, N. M.; Kenyon, J. C.; Balasubramanian, S.; Lever, A. M. *Biochemistry* **2012**, *51*, 3162.

(2) Wei, X. P.; Decker, J. M.; Liu, H. M.; Zhang, Z.; Arani, R. B.; Kilby, J. M.; Saag, M. S.; Wu, X. Y.; Shaw, G. M.; Kappes, J. C. *Antimicrob Agents Ch* **2002**, *46*, 1896.

(3) Akari, H.; Uchiyama, T.; Fukumori, T.; Iida, S.; Koyama, A. H.; Adachi, A. *J Gen Virol* **1999**, *80 (Pt 11)*, 2945.

(4) Aiken, C. *J Virol* **1997**, *71*, 5871.